Applied Surface Science 359 (2015) 236–244

Contents lists available at ScienceDirect

Applied Surface Science

journal homepage: www.elsevier.com/locate/apsusc

Crystal plasticity finite element modelling of the effect of friction on surface asperity flattening in cold uniaxial planar compression

Hejie Li[a,b,*], Andreas Öchsner[b], Dongbin Wei[a,c], Guowei Ni[d], Zhengyi Jiang[a,*]

[a] School of Mechanical, Materials and Mechatronic Engineering, University of Wollongong, NSW 2522, Australia
[b] Griffith School of Engineering, Griffith University (Gold Coast Campus), Parklands Drive, Queensland 4214, Australia
[c] School of Electrical, Mechanical and Mechatronic Systems, Faculty of Engineering and Information Technology, University of Technology, Sydney, NSW 2007, Australia
[d] Faculty of Engineering, North China University of Science and Technology, Hebei 063000, China

ARTICLE INFO

Article history:
Received 16 May 2015
Received in revised form 4 October 2015
Accepted 6 October 2015
Available online 8 October 2015

Keywords:
Crystal plasticity finite element model
Texture
Cold uniaxial planar compression (CUPC)
Flow stress
Friction

ABSTRACT

During uniaxial planar compression of annealed aluminium alloys, a novel approach to determine the surface asperity flattening (roughness R_a) is employed by analyzing the evolution of the surface's micro-texture. With an increase in compression strain, the surface asperity tends to be flattened, and strain hardening increases. Lubrication can constrain the surface asperity flattening process and hinder the progress of grain surface flattening. The development of surface texture shows an obvious dependency: under the influence of friction, the normal deformation texture component (brass orientation $\{0\,1\,1\}\langle 1\,1\,2\rangle$) can be generated easily, while lubrication can hinder this texture component generation. Simulated results show a good agreement with experimental results which predicated brass orientation. However, due to the limitation of the FCC Taylor model, the other orientation components cannot be predicted.

1. Introduction

The surface quality of metal products is an important parameter in metal forming processes. As a main factor of surface quality, the surface roughness plays a significant role in the surface quality of metal forming products. Practically, a metal forming process includes two typical processes: one is free surface evolution, in which process the sample surface does not come in contact with the tool such as stretching and tension; the other is constraint surface evolution where the sample comes in contact with the deforming tool. Therefore, the deformation is the constraint deformation such as rolling, extrusion, deep drawing, etc. [1–4]. There are a lot of references which mention free surface evolution [5–9]. However, few researchers have focused on the constraint surface evolution. In practical production, in order to improve the surface quality of metal products, the tool's surface will be manufactured much flatter and smoother than that of the metal samples. Thus, the surface evolution in constraint deformation is really a surface asperity flattening process [10–17]. Recently, Li et al. [18–20] employed crystal plasticity finite element (FE) theory in a 3D surface asperity flattening model to simulate the practical constraint deformation process, to analyze the relationship between the surface asperity and reduction, strain rate and texture. They pointed out that during the cold uniaxial planar compression (CUPC) process the surface evolution of the sample is proportional to the applied reduction. The deformation rate also plays an obvious role in the surface asperity flattening by decreasing the surface roughness and increasing the microhardness and flow stress. Furthermore, in this study, the behaviour of friction in the CUPC process is analyzed by employing a face centred cubic (FCC) rate-dependent crystal plasticity code in a 3D finite element model.

2. Experimental and sample preparation

2.1. Sample

In this study, the aluminium alloy 6061 has been chosen as the material for testing. Originally, all samples were heated in a furnace at 500 °C for 2 h, and then cooled in a furnace to room temperature. In order to generate the required surface roughness, samples were ground by sand paper no. P220. The roughness of all samples was in the following range: R_a is about 0.72 μm, R_q is about 0.84 μm, and the minimum error is around 0.02 μm.

* Corresponding authors at: School of Mechanical, Materials and Mechatronic Engineering, University of Wollongong, NSW 2522, Australia.
E-mail addresses: hejiel2003@gmail.com (H. Li), jiang@uow.edu.au (Z. Jiang).

http://dx.doi.org/10.1016/j.apsusc.2015.10.043
0169-4332/

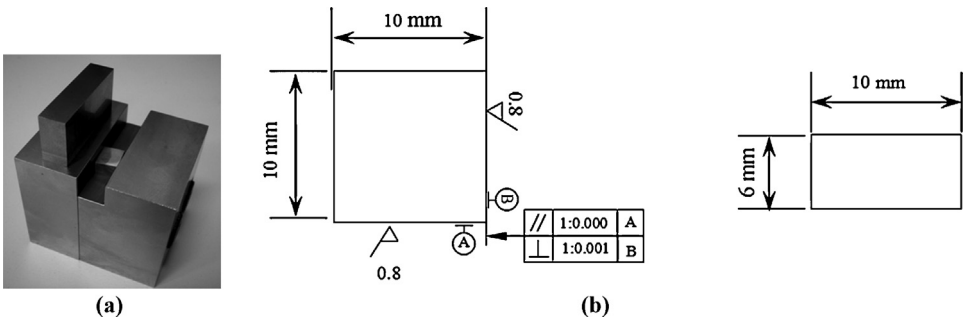

Fig. 1. Compressing equipment and sample: (a) compressing device, (b) sample [18,21]. Unit: mm.

2.2. Equipment

After a fully annealed heat treatment process (500 °C, for 2 h), aluminium alloy 6061 samples (10 mm × 10 mm × 6 mm, as shown in Fig. 1b) were compressed in a channel die, while samples were constrained in the transverse direction. In order to reduce the tool's influence, the compressing tool is polished smoothly (surface roughness R_a is about 10 nm) and flat. The gauged reduction ranges from 0 to 60%. The compression schedule is shown in Table 1. The compressing channel die includes two parts: the compressing mould and the tool (see Fig. 1a and b). For convenience of handling the sample, the compressing mould includes two separate parts which are assembled by a screw. The compression test was carried out by an INSTRON servo-hydraulic testing machine with a strain rate of about 0.001 s^{-1}.

2.3. Cold uniaxial planar compression process

The compression process was also carried out in an INSTRON material testing machine. The testing schedule is shown in Table 1 where N_i means all the samples are compressed without lubrication; L_j are the samples which are compressed with lubricants.

On the basis of static deformation, initial strain rates are chosen as 0.001 and 0.01 s^{-1}. However, in the whole deformation process, the strain rates are not the same, and it is difficult to control the strain rate on the INSTRON material testing machine. Thus, the displacement rate is used to replace the strain rate [19,20]. The calculated displacement rates are shown in Table 1. This replacement may lead to some limitations (such as errors) in the simulation. During the test, the original position and the final position of the compressing tools have been recorded. During the analysis of experimental results, the deformation of strain caused by the machine has already been subtracted. The relationship between strain rate and displacement rate can be obtained from Eq. (1):

$$H_0 = H + \Delta H, \quad \varepsilon = \ln\frac{H}{H_0}, \quad \Delta t = U/\dot{U}, \quad \dot{U} = \frac{\Delta H}{\Delta t} \tag{1}$$

where H_0, H, ΔH are the original height, the height after compression and the height increment, respectively, and where ε is the true strain, Δt is the time for deformation, and $\dot{U}$ is the displacement rate of the sample in compression.

2.4. Atomic force microscope

Before and after compression, the sample's surface morphology and roughness were measured by an atomic force microscope (AFM). The AFM maps were scanned by contact mode with the following set of parameters: scan size of 50.00 μm, scan rate of 1.5 Hz and resolution of 512. The distance between the mid-section and surface is only about 400 μm. Though the scan size of the AFM is only 50 μm × 50 μm, we also scanned nine different areas along the centre area for statistical analysis. The employed AFM result was chosen after the comparison and analysis.

2.5. Electron back-scattering diffraction

Samples were measured by electron back-scattering diffraction (EBSD) along the transverse direction (TD). AFM and EBSD were combined to analyze the relationship between the surface asperity feature and surface texture. The measuring map of cold-planar compressed samples is analyzed by the method presented in Ref. [21]. A low-angle grain boundary (LAGB) is defined as $2^\circ \le \theta < 15^\circ$ where θ is the angle of the grain orientation spread. A high-angle grain boundary (HAGB) is defined as $15^\circ \le \theta \le 62.8^\circ$. The threshold for a sub-grain is 2°. EBSD testing was conducted at the mid-section of the samples in the normal direction (ND)-rolling direction (RD), with scanning step sizes of 0.5 and 0.25 μm. The EBSD acquisition is detailed in Ref. [22].

3. Crystal plasticity finite element model

3.1. Single grain model

For crystal plasticity, the single crystal model is based on the following five assumptions [23,24]: (1) neglect of other deformation mechanisms, slip is the only one; (2) the activated slip system is $\{1\,1\,1\}\langle 1\,1\,0\rangle$; (3) twinning exists in the systems with low stack fault energy metal; (4) in the same metal, all the slip systems have the same critical shearing stress; (5) the trans-granular slip is homogeneous. The velocity gradient for the plastic deformation is given as [25–29]

$$\dot{F}^p \cdot F^{p^{-1}} = \sum_{\alpha=1}^{n} \dot{\gamma}^\alpha u_0^\alpha \otimes v_0^\alpha, \quad S_0^\alpha = u_0^\alpha \otimes v_0^\alpha \tag{2}$$

Table 1
Compression schedule.

Samples	Height (mm)	Reduction (%)	Strain rate (s^{-1})	Displacement rate (mm/min)	Displacement (mm)	Height after compression (mm)
N_1/L_1	6.3	0	0.01	0	0	6.3
N_2/L_2	6.3	20	0.01	−3.39	1.26	5.04
N_3/L_3	6.3	40	0.01	−2.96	2.51	3.79
N_4/L_4	6.3	60	0.01	−2.48	3.78	2.52